

K^+/π^+ horn: appropriate statistics for nonextensive particle production and nonequilibrium phase transition

Abdel Nasser Tawfik*

Future University in Egypt (FUE), 5th Settlement, 11835 New Cairo, Egypt

Eman R. Abou Elyazeed and Hayam Yassin

Physics Department, Faculty of Women for Arts,

Science and Education, Ain Shams University, 11577 Cairo, Egypt

(Dated: March 18, 2022)

We suggest that the long-standing problem with incapability of the thermal models in reproducing the horn-like structure of the kaon-to-pion ratio measured at AGS, SPS and low RHIC energies and confirmed in the beam energy scan program, was raised due to applying inappropriate statistics, mainly, extensive additive Boltzmann-Gibbs (BG). The assumption that the particle production, the dynamical nonequilibrium process, is *priori* to be analyzed by extensive BG or nonextensive Tsallis statistics, seems being a failed path followed over the past decades. With generic (non)extensive statistics, two equivalence classes (c, d) belittle such an *ad hoc* assumption. Accordingly, the statistical ensemble itself determines its degree of (non)extensivity, including extensive BG and nonextensive Tsallis statistics, which are characterized by $(1, 1)$ and $(0, q)$, respectively. The energy dependence of light-, γ_q , and strange-quark occupation factor, γ_s , indicates that the produced particles are best described as a nonequilibrium ensemble, where a remarkable non-monotonic behavior associates the K^+/π^+ horn, for example. On other hand, the resulting equivalence classes (c, d) refer to a generic nonextensivity associated with extended exponential and Lambert- W_0 exponentially generating distribution function, which obviously emerge from free, short- and long-range correlations. With this generic statistical approach, the hadron resonance gas model excellently reproduces the K^+/π^+ ratio, including its nonmonotonic horn-like structure.

Keywords: Nonequilibrium and irreversible thermodynamics, Self-organized systems, Relativistic heavy-ion collisions, Other topics in statistical physics, thermodynamics, and non-linear dynamical systems

I. Introduction

A nonmonotonic horn-like structure of the K^+/π^+ ratio was confirmed in various experiments, at AGS, SPS and low RHIC energies [1–5]. At $\sqrt{s_{NN}} \lesssim 20$ GeV, there is a monotonic rapid increase followed by a monotonic rapid decrease, i.e., a maximum appears, while at energies $\gtrsim 20$ GeV, the RHIC and LHC energies, the K^+/π^+ ratio seems to be nearly energy-independent, i.e., a plateau is formed. Various interpretations have been given in literature [1, 6–12]. The thermal models which are either based on extensive additive Boltzmann–Gibbs (BG) and/or on Tsallis-type nonextensive statistics [13] aren't well succeeded in reproducing the nonmonotonic horn-like structure of the K^+/π^+ ratio, Fig. 4 and Fig. 3. Despite of this, various extensions to the thermal models are allegedly assumed to deliver explanations for the underlying processes in the particle production [14–20]!

To improve the capability of the thermal models; the ideal gas of identified hadronic resonances, one of the authors (AT) proposed i) a substantial change in the single-particle distribution function due to a dynamical change in the phase-space volume, especially at the phase transition, whose imprints seem to survive till the chemical freezeout, where the produced particles are detected [11], ii) integrating nonequilibrium light- and strange-quark occupation factors, $\gamma_{q,s}$, in the phase-space volume [8, 21, 22], iii) applying Tsallis-type nonextensive statistics [13], and iv) deriving the ideal gas of hadron resonances away from equilibrium by assigning *eigen*-volume to each of its constituents [23, 24]. Castorina *et al.* assumed a suppression in the strange-quark occupation factor, γ_s , that accounts for reducing the production rates of the strange particles in pp , pA , AA collisions, at different energies and found that the strangeness suppression disappears with the onset of the color deconfinement and full-chemical nonequilibrium is subsequently attained [25, 26]. The occupation factors, $\gamma_{q,s}$, introduce controllers over the numbers of light- and strange-quarks fitting within the phase-space element, i.e., a similar role as that of the chemical potentials. None of these ingratiatees was able to satisfactorily

*Electronic address: a.tawfik@fue.edu.eg

reproduce the various particle ratios, including K^+/π^+ [21, 22, 27].

Hence, there is a conceptual reason. Imposing nonequilibrium (either as partial- or full-chemical nonequilibrium $\gamma_{q,s}$ or as finite sizes of the constituents of the ideal gas, etc.) in an equilibrium ensemble of BG-type extensive additive statistics seems conceptually unsuccessful. Even if Tsallis-type nonextensivity is assumed, the matching of nonequilibrium with nonextensivity would be improved, on one hand. On the other hand, the price to be paid in return is huge. This isn't less than lose the meaning of the thermodynamic quantities, such as the freezeout temperature [28–30]. With this regard, it should be highlighted that the Tsallis-type nonextensivity is limited to a one-dimensional line within the entire space of (non)extensivity utilized in present calculations, in which both BG and Tsallis statistics are merely special cases.

The relativistic high-energy collisions are assumed to go through several *critical* processes, such as deconfinement and hadronization. A radical change in properties, symmetries, and degrees of freedom (dof) of the QCD matter is obviously depending on the collision energy. The horn-like structure of the kaon-to-pion ratio, which normalizes strange to light quark flavors, likely signals onset of nonextensive particle production and nonequilibrium phase transition that might dynamically enhance the strange quark flavor or suppress the light quark flavor or vice versa. The present script suggests that the incapability of the *extensive additive* thermal models in reproducing the horn-like structure measured at AGS, SPS and low RHIC energies, Fig. 4 and Fig. 3, is due to inappropriate statistics. Generic (non)extensive statistics, section II, autonomously describes the equivalence classes of the *generalized* entropies in the entire (c, d) -plane [31]. At the chemical freezeout, where detection of the produced particles takes place, the statistical ensemble is therefore dynamic and probably violates the fourth Shannon–Khinchin axiom [30]. Even if this wouldn't be the case and the produced particles would be in full-chemical nonequilibrium, generic (non)extensive statistics is also well applicable. Extensive or nonextensive ensemble and equilibrium or out-of-equilibrium system are properly encoded by the equivalence classes (c, d) including extensive BG and Tsallis-type nonextensive statistics, which are characterized by $(c, d) = (1, 1)$ and $(c, d) = (0, q)$, respectively.

We first assume partial-chemical nonequilibrium in generic (non)extensive statistics, i.e., $\gamma_q = 1$, while γ_s is to be determined from the statistical fit of various particle ratios, in a wide range of energies, to the available experimental measurements. We also assume full-chemical nonequilibrium, i.e., both $\gamma_q \neq 1$ and $\gamma_s \neq 1$ are determined from the statistical fits, as well. In the same manner, the energy-dependence of the equivalence classes (c, d) is also determined, Fig. 1. In the present script, the occupation factors $\gamma_{q,s}$, the equivalence classes (c, d) , and the

freezeout parameters; the temperature T and the baryon chemical potential μ_B , aren't fitting variables. They are inputs varying with the collision energies. With these inputs, the K^+/π^+ ratio calculated in generic (non)extensive statistics excellently reproduces its measured result including the nonmonotonic horn-like structure, at $\sqrt{s_{NN}} \lesssim 20$ GeV; the AGS, SPS and low RHIC energies, Fig. 3.

The present paper is organized as follows. The generic (non)extensive approach is reviewed in section II. The energy-dependence of the equivalence classes (c, d) , the light- and strange-quark occupation factors $\gamma_{s,q}$, and the K^+/π^+ ratio is presented in section III A, III B, and III C, respectively. Section IV is devoted to the conclusions. Appendices A, B and C respectively elaborate details on probability distribution, entropy, and exponential and logarithm functions in Boltzmann, Tsallis, and generic (non)extensive statistics, The impacts of the inclusion of very high-mass resonances and missing states in the hadron resonance gas model, and the contour plots of the quality of fit for $\gamma_{q,s}$. The quality of the fit for the equivalence classes (c, d) is depicted in Fig. 1.

II. Generic (non)extensive statistical approach

In generic (non)extensive statistics, the partition function can be given as [27, 32]

$$\ln Z(T, \mu) = \pm V \sum_i \frac{g_i}{(2\pi)^3} \int_0^\infty \ln [1 \pm \varepsilon_{c,d,r}(x_i)] d^3 \mathbf{p}, \quad (1)$$

where $x_i = [\mu_i - E_i(\mathbf{p})]/T$ with $E_i(p) = \sqrt{\mathbf{p}^2 + m_i^2}$; the dispersion relation of i -th particle, μ_i is the chemical potential of that particle; $\mu_i = B_i\mu_B + S_i\mu_S + \dots$, with S_i and B_i are the corresponding strangeness and baryon quantum numbers and μ_S and μ_B are the strangeness and baryon chemical potential, respectively. g is the degeneracy factor, V is the volume of the fireball, \mathbf{p} is the momentum, and \pm represent fermions and bosons, respectively. The extended exponential function $\varepsilon_{c,d,r}(x_i)$ is given as [31, 33]

$$\varepsilon_{c,d,r}(x_i) = \exp \left[\frac{-d}{1-c} \left(W_k \left[B \left(1 - \frac{x_i}{r} \right)^{\frac{1}{d}} \right] - W_k[B] \right) \right], \quad (2)$$

where W_k is the Lambert- W_k function which has real solutions, at $k = 0$ with $d \geq 0$, and at $k = 1$ with $d < 0$.

$$B = \frac{(1-c)r}{1-(1-c)r} \exp \left[\frac{(1-c)r}{1-(1-c)r} \right], \quad (3)$$

where $r = (1 - c + cd)^{-1}$ with c, d are two critical exponents defining the equivalence classes for both types of extensive and nonoextensive statistical ensembles. The latter are statistical

systems violating the fourth Shannon-Khinchin axiom; the generalized Shannon additivity¹, especially in their large size limit, in which two asymptotic properties of the generalized entropies are associated with one scaling function each. Each of the scaling functions is characterized by one exponent defining equivalence relations of the entropic forms, i.e., two entropic forms are equivalent if their exponents are the same.

The equivalence classes (c, d) which are two exponents determining two scaling functions with two asymptotic properties, are intrinsic properties of all types of the underlying statistics. For instance, extensive BG and Tsallis-type nonextensive statistics assume $(c, d) = (1, 1)$ and $(0, q)$, respectively [33]. The remaining c - d space is inhabited by various types of nonextensivity or superstatistics enabling us to reveal nonequilibrium phenomenon such as critical endpoint, correlations, fluctuations, higher-order cumulants, etc. The present script suggests that the horn of the kaon-to-pion ratio likely signals onset of nonextensive particle production and impact of nonequilibrium phase transition. The incapability of the *equilibrium* thermal models in reproducing the enhancement in both particle yields, the kaons and the pions, Fig. 4 and Fig. 3, could be interpreted due to inappropriate statistics [11, 23, 27, 30, 32], i.e., either extensive BG or Tsallis-type nonextensive statistics.

With the occupation factors of light- and strange-quarks, γ_q and γ_s , respectively, the generic (non)extensive partition function reads

$$\ln Z(T, \mu) = \pm V \sum_i \frac{g_i}{(2\pi)^3} \int_0^\infty \ln [1 \pm (\gamma_q^{n_q})_i (\gamma_s^{n_s})_i \varepsilon_{c,d,r}(x_i)] d^3 \mathbf{p}, \quad (4)$$

where n_q and n_s are the number of light and strange quarks, respectively². As BG statistics assumes extensivity, additivity, and equilibrium particle production, γ_q and γ_s could plainly be seen as additional variables imposed on BG statistics. But they are essential ingredients to (non)extensive statistics³. In generic (non)extensive statistics, the degree of nonextensivity

¹ If $p_{ij} \geq 0$, $p_i = \sum_{j=1}^{m_i} p_{ij}$ and $\sum_{i=1}^n p_i = 1$, where $i = 1, \dots, n$ and $j = 1, \dots, m_i$, then $S(p_{11}, \dots, p_{nm_n}) = S_1(p_1, \dots, p_n) + \sum_{i=1}^n p_i S_1\left(\frac{p_{i1}}{p_i}, \dots, \frac{p_{im_i}}{p_i}\right)$. Accordingly, S_n is the Shannon entropy given by $S_n(P) = \tau \cdot \sum_{k=1}^n p_k \log_2 p_k$ with $\tau < 0$, i.e., the entropy of a system, which could be divided into sub-systems A and B is given as S_A and the expectation value of S_B but conditional on A ; $S_{nm}(AB) = S_n(A) + S_m(B|A)$, where $S_m(B|A) = \sum_k p_k \cdot S_m(B_k)$ [32]. The generalized entropy reads $S_{c,d}[p] \propto \sum_{i=1}^\Omega \Gamma(d+1, 1-c \log(p_i))$, where the constants (c, d) characterize the universality class of entropy of the system completely in the thermodynamic limit and also specifies its distribution functions. The fourth Shannon-Khinchin axiom is corresponding to Markovian processes, which are random processes, whose future is independent of the past, and the natural stochastic analogy of the deterministic processes described by differential equations.

² Since we are interested on the QCD phase diagram, the contributions of the heavier quarks could be neglected.

³ This should not necessarily be limited to the Tsallis-type. The entire c - d space characterizes various types

shall subjectively be determined by the changeable statistical nature of the system of interest, at various energies.

With this regard, we recall that the statistical properties of an ensemble consisting of individual objects is given by a single-particle distribution function. The probability of finding an object in infinitesimal region of the phase-space is proportional to the volume of the phase-space element and the single-particle distribution function. The latter is assumed to fulfill the Boltzmann-Vlasov (BV) master equation, which is the semi-classical limit of a time-dependent Hartee-Fock theory through the Wigner transform of the one-body density matrix and can be used to study the dynamics of the constituents. At high energies, the phase-space volume and its configurations are apparently modified. So does the single-particle distribution function [11].

The occupation factors $\gamma_{q,s}$ act as controllers over the number of the quarks fitting within the phase-space element, i.e., similar to the chemical potentials $a = \ln E - \ln T - \ln N$, where $\lambda = \exp(-a)$ [34]. At $\gamma_s = \gamma_q = 1$, the statistical ensemble refers to a system in chemical and thermal equilibrium, but if γ_s or γ_q varies from unity, while its counterpart remains equilibrium, the statistical system is modified to partial-chemical nonequilibrium. At $\gamma_s \neq 1$ and $\gamma_q \neq 1$, the statistical ensemble is apparently out-of-equilibrium.

In the thermodynamic limit, the number density can then be deduced from the partition function, Eq. (4) [27, 35],

$$n(T, \mu) = \pm \sum_i \frac{g_i}{2\pi^2} \int_0^\infty \frac{(1-c)^{-1} (\gamma_q^{n_q})_i (\gamma_s^{n_s})_i \varepsilon_{c,d,r}(x_i) W_0 \left[B(1 - \frac{x_i}{r})^{\frac{1}{d}} \right]}{\left[1 \pm (\gamma_q^{n_q})_i (\gamma_s^{n_s})_i \varepsilon_{c,d,r}(x_i) \right] (r - x_i) \left(1 + W_0 \left[B(1 - \frac{x_i}{r})^{\frac{1}{d}} \right] \right)} \mathbf{p}^2 d\mathbf{p}. \quad (5)$$

At the chemical freezeout, which in both extensive BG [6, 7, 36–38] and genertic (non)extensive statistics [27] is thermodynamically conditioned along the entire QCD phase diagram, the various hadron resonances decay either to stable particles, n_i^{direct} , or to other resonances n_j . In the final state, we take this into account so that a specific particle yield, such as pion and kaon, is determined as

$$\langle n_i^{final} \rangle = \langle n_i^{direct} \rangle + \sum_{j \neq i} b_{j \rightarrow i} \langle n_j \rangle, \quad (6)$$

where $b_{j \rightarrow i}$ is the branching ratio for the decay of j -th resonance to i -th particle.

In the present work, we first assume partial-chemical nonequilibrium, i.e., $\gamma_q = 1$, while γ_s is determined from the statistical fits of the generic (non)extensive calculations of the K^+/π^+

of superstatistics including extensive and nonextensive ensembles.

ratio, in a wide range of center-of-mass energies $\sqrt{s_{NN}}$ to available experimental measurements, Fig. 2 panel (a). We also assume full-chemical nonequilibrium, i.e., both $\gamma_q \neq 1$ and $\gamma_s \neq 1$ are determined from the same statistical fits of the K^+/π^+ ratio, Fig. 2 panels (b) and (c). The degree of (non)extensivity is autonomously determined by the statistical ensemble. The results shall be discussed in the next section.

III. Results

By statistical fits of various particle ratios, at the chemical freezeout ⁴, whose parameters T and μ_B are well expressed as functions of the collision energies and thermodynamically conditioned, for example constant entropy density $s/T^3 = 7$, in either extensive BG [24, 36–38] or generic (non)extensive statistics [27], the energy dependence of the equivalence classes (c, d) , section III A, and that of the light- and strange-quark occupation factors γ_q and γ_s , section III B, have been determined in generic (non)extensive statistics, at various center-of-mass energies $\sqrt{s_{NN}}$. The three sets of parameters, the freezeout parameters, the equivalence classes and the occupation factors, enter our calculations for K^+/π^+ ratio as inputs. At a given $\sqrt{s_{NN}}$, which is related to μ_B and a freezeout temperature T , the corresponding equivalence classes and occupation factors are substituted in Eq. (5), which together with Eq. (6) determine the number density of a specific particle.

A. Equivalence classes (c, d) and nonextensivity

In Fig. 1, the resulting equivalence classes (c, d) , at various energies [27], are respectively depicted as squares and circles. These results could be well parameterized by the following expressions:

$$c(\sqrt{s_{NN}}) = \left[a_1 + (\sqrt{s_{NN}})^{-b_1} \right]^{-c_1} d_1 \sqrt{s_{NN}}, \quad (7)$$

$$d(\sqrt{s_{NN}}) = \left[a_2 - (\sqrt{s_{NN}})^{-b_2} \right]^{c_2} \exp\left(\frac{d_2}{\sqrt{s_{NN}}}\right), \quad (8)$$

where $a_1 = 1.005 \pm 0.01$, $b_1 = 3.242 \pm 0.106$, $c_1 = 3.247 \pm 0.24$, $d_1 = 6.526 \times 10^{-06} \pm 1.003 \times 10^{-06}$, $a_2 = 1.947 \pm 0.0006$, $b_2 = 0.008 \pm 0.00015$, $c_2 = 3.493 \pm 0.0739$, and $d_2 = 0.506 \pm 0.019$. Both expressions are respectively depicted as dashed and solid curves in Fig. 1.

⁴ At which the various quantum numbers, including baryon, strangeness, and electric charge, are conserved.

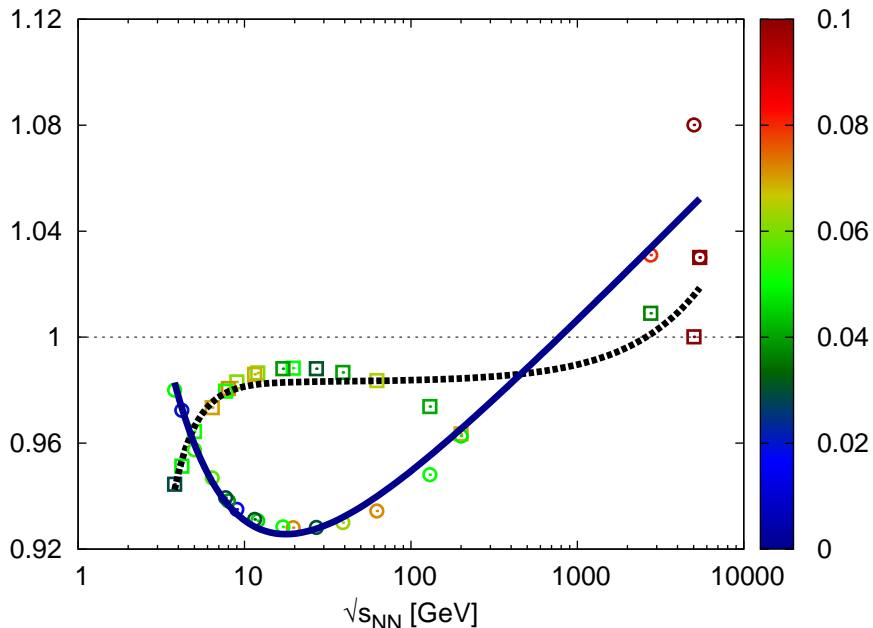


Fig. 1: Contour plot showing the equivalence classes (c, d) as functions of $\sqrt{s_{NN}}$. The dashed curve stands for c , Eq. (7), while the solid curve represents d , Eq. (8). The horizontal line refers to extensive BG statistics. The thin dashed line marks the well-defined equivalence classes of extensive BG statistics, $(c, d) = (1, 1)$. The colored band to the left illustrates the corresponding statistical errors.

At AGS energies, we find that d seems to start from a large value (nearly unity) and rapidly decreases, while c starts from ~ 0.94 and exponentially increases with increasing energy. At $\sqrt{s_{NN}} \simeq 4 \pm 1$ GeV, the values of both equivalence classes become equal, $(c, d) \simeq (0.97, 0.97)$. At SPS and low RHIC energies, another remarkable conclusion can be drawn. While c reaches a maximum value, at $\sqrt{s_{NN}} \simeq 10 \pm 1$ GeV, d continues its decrease and approaches its minimum $d \sim 0.93 \pm 0.02$, at $\sqrt{s_{NN}} \simeq 20 \pm 2$ GeV. At RHIC and LHC energies, c sets on a wide plateau, at $c \simeq 0.985$. At $\sqrt{s_{NN}} \gtrsim 20$ GeV, d switches to a nice exponential increase with increasing energy. c turns to set on such an exponential increase, at LHC energies, where both equivalence classes exceed the unity, i.e., the second Shannon–Khinchin axiom also becomes violated.

The degree of (non)extensivity is to be determined by the equivalence classes (c, d) , whose energy-dependence was best parameterized by Eqs. (7) and (8), respectively, and depicted in Fig. 1. We notice that the resulting equivalence classes are positive and close to unity. This means that:

1. the underlying statistics isn't extensive BG, especially at AGS and SPS energies, but

certainly not Tsallis–type nonextensive statistics,

2. at AGS, SPS and RHIC energies, the statistical systems holds first ⁵, second ⁶ and third ⁷ Shannon–Khinchin axioms but violates the fourth Shannon–Khinchin axiom,
3. at LHC energies, both second and fourth Shannon–Khinchin axioms are violated, and d) the corresponding entropy is Lambert– W_0 exponential; exponentially generating function $W_0(x) = \sum_{n=1}^{\infty} (-n)^{n-1} x^n / n!$.

Even the slight difference from unity depicted in Fig. 1, the resulting (c, d) play an essential role by deriving the entire statistical system from extensivity, additivity, and equilibrium. Boltzmann statistics is sharply located at $(c, d) = (1, 1)$. Any deviation from $(c, d) = (1, 1)$ apparently replaces Boltzmann distribution, entropy, exponential, and logarithm functions by their counterparts characterizing generic (non)extensive statistics, Appendix A. The extended exponential and Lambert– W_0 exponentially generating distribution function, are substantially different from the ordinary exponential and distribution functions.

B. Nonequilibrium quark occupation factors

In partial– and full–chemical nonequilibrium, various particles ratios measured, at various $\sqrt{s_{NN}}$, are fitted to their calculations in generic (non)extensive statistics. At a given $\sqrt{s_{NN}}$, the corresponding equivalence classes (c, d) , section III A, and freezeout parameters μ_B and T are substituted in the expression for the number density of a specific particle yield. With the fitting parameters either γ_s , at $\gamma_q = 1$ for partial–chemical nonequilibrium or γ_s and γ_q for full–chemical nonequilibrium various particles ratios calculated in generic (non)extensive statistics are fitted to the measured ones. The overall energy dependence of both γ_q and γ_s , Fig. 2, is given as

$$\gamma_{s,q}(\sqrt{s_{NN}}) = \alpha \exp(-\beta \sqrt{s_{NN}}) \sin(\nu \sqrt{s_{NN}} + \eta) + \zeta, \quad (9)$$

⁵ The Shannon entropy $S_n(p) = -\tau \cdot \sum_{k=1}^n p_k \log_2 p_k$, where $\tau < 0$, is continuous in Δ_n . i.e., the entropy continuously depends on p .

⁶ For the uniform distribution $U_n = (1/n, \dots, 1/n) \in \Delta_n$, the Shannon entropy is maximum, i.e., $S_n(p) \leq S_n(U_n)$ for any $p \in \Delta_n$ [32].

⁷ The Shannon entropy is expandable; $S_{n+1}(p_1, p_2, \dots, p_n, 0) = S_n(p_1, p_2, \dots, p_n)$ for all $(p_1, p_2, \dots, p_n) \in \Delta_n$, i.e., the requirement that adding a zero–probability state to a system does not change the entropy.

where the values of the parameters α , β , ν , η , ζ distinguish between partial- ($\gamma_q = 1$ while γ_s is the fitting variable) and full-chemical nonequilibrium, Tab. I.

| nonequilibrium | | α | β | ν | η | ζ |
|---------------------------|------------|--------------------|-------------------|--------------------|-------------------|-------------------|
| partial at $\gamma_q = 1$ | γ_s | 10.373 ± 0.625 | 0.361 ± 0.009 | 0.233 ± 0.003 | 5.362 ± 0.014 | 0.751 ± 0.018 |
| full | γ_s | 2.913 ± 0.259 | 0.262 ± 0.062 | -0.257 ± 0.018 | 4.353 ± 0.081 | 0.804 ± 0.025 |
| | γ_q | -5.264 ± 0.256 | 0.381 ± 0.018 | 0.373 ± 0.017 | 4.88 ± 0.071 | 1.037 ± 0.041 |

Tab. I: Fitting parameters of the dependence of $\gamma_{s,q}$ on $\sqrt{s_{NN}}$, Eq. (9).

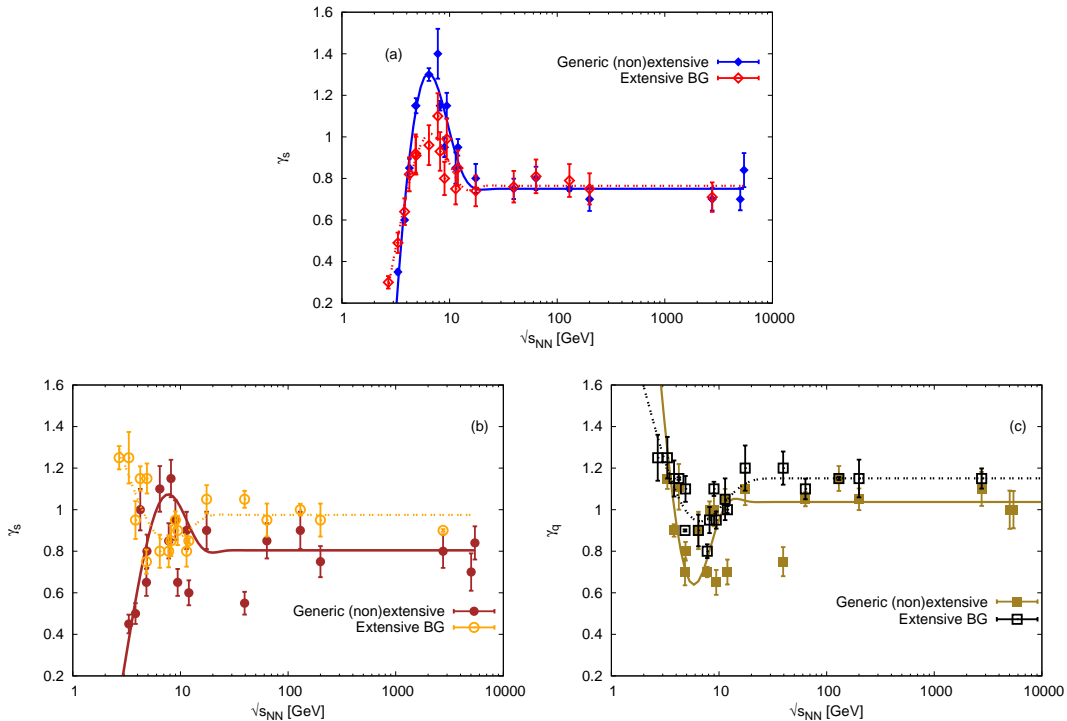


Fig. 2: Top panel (partial-chemical nonequilibrium): γ_s is given as a function of $\sqrt{s_{NN}}$, where $\gamma_q = 1$. Bottom panel (full-chemical nonequilibrium): both γ_s (left) and γ_q (right) are the fitting variables. Solid symbols with errors depict our results from the statistical fits of the measured K^+/π^+ with the generic (non)extensive calculations. Open symbols with errors represent the statistical fits of the measured K^+/π^+ to the extensive BG statistics [22]. The solid and double-dotted curves show Eq. (9) of the present study and refs. [21, 22], respectively.

The dependence of γ_s and γ_q on $\sqrt{s_{NN}}$ is presented in Fig. 2. The solid symbols refer to the present results from the statistical fits of the measured K^+/π^+ ratio to the generic

(non)extensive calculations, Eq. (5), while the open symbols represent the calculations from the extensive hadron resonance gas (HRG) model based on extensive BG statistics [21, 22]. Top panel of Fig. 2 shows γ_s in dependence on $\sqrt{s_{NN}}$ as calculated in generic (non)extensive statistics, where $\gamma_q = 1$, i.e., partial-chemical nonequilibrium. Bottom panel of Fig. 2 depicts the dependence of γ_s (left panel) and γ_q (right panel) on $\sqrt{s_{NN}}$, i.e., full-chemical nonequilibrium. The proposed expression, Eq. (9), based on generic (non)extensive statistics for the dependence of γ_s and/or γ_q on $\sqrt{s_{NN}}$ is depicted by solid curves. The double-dotted curves are the corresponding expressions deduced from the extensive HRG model, which is based on extensive BG statistics [21, 22].

In top panel of Fig. 2, at $\gamma_q = 1$ and partial-chemical nonequilibrium, we notice that γ_s exponentially increases, at $\sqrt{s_{NN}} \lesssim 7$ GeV. The same behaviour was quantitatively observed in the extensive BG calculations [21]. The rate of increase in the present calculations (generic (non)extensive statistics) is larger than in extensive BG statistics. At higher energies ($7 \lesssim \sqrt{s_{NN}} \lesssim 20$ GeV), γ_s rapidly decreases. Also here, the rate of decreasing γ_s in generic (non)extensive statistics is larger than that in extensive BG statistics. At $\sqrt{s_{NN}} > 20$ GeV, γ_s becomes energy independent. At this plateau, the resulting γ_s from both types of statistics is in good agreement with each other, $\gamma_s \simeq 0.78 \pm 0.01$. We conclude that with the global assumption that $\gamma_q = 1$, the resulting γ_s equally encodes the partial-chemical nonequilibrium in both types of statistics, at $\sqrt{s_{NN}} > 20$ GeV. At lower energies, both types of statistics significantly disagree with each other, especially at $\sqrt{s_{NN}} \simeq 7$ GeV. Here, the generic (non)extensive γ_s is $\sim 40\%$ larger than the extensive BG γ_s , i.e., the partial-chemical nonequilibrium in strange-quark occupation factor is $\sim 40\%$ larger. In other words, the signals for the strangeness enhancement, for instance, at the peak (horn) of the kaon-to-pion ratio, are more than 40% overcast shrouded when measurements, such as multiplicity of the produced particles, are restricted to extensive BG statistics. Hence, a recommendation to the fellow experimentalists can be now addressed. Applying generic (non)extensive statistics, especially in Run II of the STAR beam energy scan program [39, 40], and the future facilities, FAIR and NICA, likely exposes essential experimental signals.

Bottom panel of Fig. 2 shows nonequilibrium γ_s (left) and γ_q (right). In bottom left panel, we notice that at $\sqrt{s_{NN}} \lesssim 7$ GeV and varying γ_q , γ_s calculated from generic (non)extensive statistics exponentially increases with increasing $\sqrt{s_{NN}}$, while γ_s deduced from the extensive HRG calculations exponentially decreases [22]. It is apparent that the rate of the increase in the earlier is more rapid than that of the decrease in the latter. Also here, we find that both

maximum [generic (non)extensive statistics] and minimum (BG statistics) are likely positioned, at $\sqrt{s_{NN}} \simeq 7$ GeV. At $7 \lesssim \sqrt{s_{NN}} \lesssim 20$ GeV, the generic (non)extensive γ_s rapidly decreases, while the extensive BG γ_s rapidly increases.

At $\sqrt{s_{NN}} > 20$ GeV, γ_s from both types of statistics becomes energy independent. Opposite to the partial-chemical nonequilibrium (top panel), the corresponding plateaus are not coincident. While the extensive BG $\gamma_s \simeq 0.98 \pm 0.1$, i.e., very close to equilibrium, the generic (non)extensive $\gamma_s \simeq 0.81 \pm 0.01$ referring to large nonequilibrium. To draw a conclusion about the degree of (non)equilibrium, the resulting γ_q which is depicted in the bottom left panel should also be taken into consideration. Relative to the plateaus formed, at high energies, we notice that the height of the γ_s crest [generic (non)extensive] is larger than the depth of the γ_s trough [extensive BG], at $\sqrt{s_{NN}} \simeq 7$ GeV.

The bottom right panel of Fig. 2 depicts the energy dependence of γ_q , at varying γ_s . Here, we find that at $\sqrt{s_{NN}} \lesssim 7$ GeV, both generic (non)extensive γ_q and extensive BG γ_q (HRG model) exponentially decrease with increasing energy. The rate of the earlier is larger than that of the latter. While both minima are nearly positioned, at $\sqrt{s_{NN}} \simeq 7$ GeV, their depths aren't the same. The depth of the generic (non)extensive γ_q is larger than that of the extensive BG γ_q . Also, γ_q becomes energy independent, at $\sqrt{s_{NN}} > 20$ GeV. The heights of both plateaus aren't coincident. The generic (non)extensive are lower than the extensive BG results. We find that, both generic (non)extensive extensive BG $\gamma_q > 1$.

Both bottom panels illustrate that a) the resulting values of γ_q and γ_s obtained from generic (non)extensive statistics are lower than their values in extensive BG statistics, b) at $\sqrt{s_{NN}} \lesssim 7$ GeV, there is an exception that the generic (non)extensive γ_s reaches maximum, c) the span of the values that γ_q and γ_s take in extensive BG statistics is narrower than in generic (non)extensive statistics, and d) at $\sqrt{s_{NN}} \gtrsim 20$ GeV, both generic (non)extensive extensive BG $\gamma_{q,s}$ are nearly energy-independent, where $\gamma_q > 1$ and $\gamma_s < 1$.

C. K^+/π^+ ratio

Figure 3 depicts the K^+/π^+ ratio as a function of $\sqrt{s_{NN}}$. Symbols refer to the experimental results, at energies ranging from 5 GeV to 5.44 TeV [2–5, 41–45]. The dotted curve shows the generic (non)extensive calculations, at partial-chemical nonequilibrium, i.e., varying γ_s , while $\gamma_q = 1$. The solid curve illustrates the results, at full-chemical nonequilibrium, i.e., varying γ_s and γ_q . The double-dashed curve gives the extensive BG calculations, at partial-

chemical nonequilibrium [21], while the dashed curve presents the extensive BG calculations, at full-chemical nonequilibrium [22]. The incapability of the equilibrium HRG model, i.e., $\gamma_q = \gamma_s = 1$, in reproducing both the horn-structure of the K^+/π^+ ratio, at AGS, SPS, and low RHIC energies, and their measurements, at RHIC and LHC energies, is shown by the long-dashed curve.

In the HRG model; an ideal gas of point-like hadrons characterized by the Hagedorn mass spectrum which is consisting of a discrete (so-far measured) and a continuous (missing hadron states), various higher-order thermodynamic quantities have been analyzed [46]. In a previous study [47], one of the authors (AT) concluded that the missing states aren't considerably contributing to the lower-order thermodynamic quantities, especially the first-order ones, the particle number or particle multiplicity. Thus, the inclusion of missing states wouldn't improve the thermal model incapability to reproduce the horn-structure of the K^+/π^+ ratio, Appendix B.

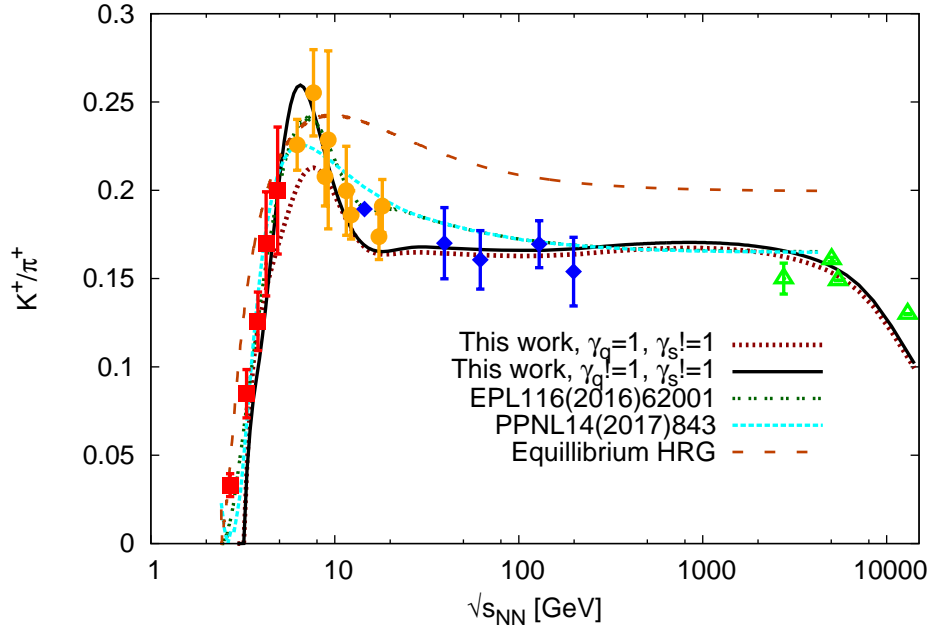


Fig. 3: The experimental results of the K^+/π^+ ratio are given in dependence on $\sqrt{s_{NN}}$ [2–5, 41–45]. The solid and dotted curves depict the generic (non)extensive calculations, at full- (γ_q and $\gamma_s \neq 1$) and partial-chemical nonequilibrium ($\gamma_s \neq 1$), respectively. Double-dashed and dashed curves represent the extensive BG results, at full- [21] and partial-chemical nonequilibrium [22]. The long-dashed curve shows the HRG calculations, at equilibrium, i.e., $\gamma_q = \gamma_s = 1$.

We find that the generic (non)extensive calculations in the entire energy spectrum excellently

agree with the experimental results. The horn-like structure of the kaon-to-pion ratio is perfectly reproduced. Comparing to the other types of statistics, the generic (non)extensive approach is well capable in describing the rapid increase, at $\sqrt{s_{NN}} \lesssim 7$ GeV and also the fast decrease, at $7 \lesssim \sqrt{s_{NN}} \lesssim 20$ GeV. At $\sqrt{s_{NN}} \gtrsim 20$ GeV, a fine structure of the plateau is predicted. Because of the wide gap between top RHIC and LHC energies, this is an essential estimation. Another finding is that both partial- and full-chemical nonequilibrium results significantly vary, especially at $\sqrt{s_{NN}} \lesssim 7 \pm 1$ GeV. This emphasizes that the light quark occupation factor, γ_q becomes significant, at $\sqrt{s_{NN}} \lesssim 7 \pm 1$ GeV. As depicted in bottom right panel of Fig. 2, at this energy, γ_q becomes minimum, while γ_s reaches a maximum. The span between both values increases when moving from partial- to full-chemical nonequilibrium. So does the horn of the kaon-to-pion ratio. In light of this, we conclude that the horn-structure of the kaon-to-pion ratio is likely due to a) Lambert- W_0 exponentially generating distribution function [generic (non)extensive statistics] and b) full-chemical nonequilibrium quark occupation factors.

The full-chemical nonequilibrium predicts a further enhancement in the K^+/π^+ ratio, especially at $3 \lesssim \sqrt{s_{NN}} \lesssim 10$ GeV. At these energies, a detailed beam energy scan by the STAR and the CBM experiments, for instance, is recommended to refine the conclusion whether partial- or full-chemical nonequilibrium excellently reproduces the nonmonotonic horn-structure of the K^+/π^+ ratio, at AGS, SPS and low RHIC energies.

IV. Conclusion

The present paper introduces generic (non)extensive statistics. The physical motivation isn't just to propose an approximate solution to a long-standing problem, the failure of thermal models in reproducing the nonmonotonic horn-like structure of the K^+/π^+ ratio. The assumption that the particle production could be analyzed by extensive additive equilibrium statistics is badly contradicts the nature of the high-energy particle production. On one hand, this could be tolerated as long as no other alternative existed. The nonextensive Tsallis approach is a very special case and seems to fail, as well. The present paper introduces a first-principle solution based on proper statistical approach, namely statistics whose extensivity and nonextensivity match well with the statistical nature of the particle production.

Various ingredients, such as modifying single-particle distribution function [11], assuming nonequilibrium light- and strange-quark occupation in the phase-space volume, i.e., $\gamma_{q,s} \neq 1$

[8, 21, 22], and integrating an *excluded* volume in the *pointlike* ideal gas of hadron resonances [23, 24], have been introduced to improve the capability of the thermal approaches, which are either based on extensive additive BG statistics [1, 6–12] or on Tsallis–type nonextensive statistics [13]. These weren’t fully succeeded in characterizing the particle ratios including the nonmonotonic horn–like structure of the K^+/π^+ ratio, which likely signals onset of nonextensive particle production and impacts of nonequilibrium phase transition.

The present script assumes that the incapability of the thermal models in reproducing the horn–like structure (long–dashed curve in Fig. 3) is due to inappropriate statistics; either extensive additive BG or Tsallis–type nonextensive statistics or their extensions. Inserting nonequilibrium ingredients such as modified single–particle distribution function or nonequilibrium occupation factors $\gamma_{q,s}$ or finite volume of the constituents of the ideal gas to extensive additive BG statistics is conceptionally fruitless. But these are eligible in nonextensivity statistics. Relative to the entire c – d space of (non)extensivity, the Tsallis–type nonextensivity is limited to a line, where $c = 0$ and $d = q$. On the other hand, generic (non)extensive statistics covers the entire space of the two equivalence classes (c, d) . With this statistical approach, the ensemble itself determines its statistical extensivity and nonextensivity. Even both extensive BG and Tsallis–type nonextensive statistics are included in. They are sharply characterized by $(1, 1)$ and $(0, q)$, respectively.

First, the partial– and full–chemical nonequilibrium, γ_q or/and γ_s have been determined, at different energies. Second, in the same manner, the energy–dependence of (c, d) are estimated. In calculating the K^+/π^+ ratio, the occupation factors $\gamma_{q,s}$, the equivalence classes (c, d) , and the freezeout parameters (T, μ_B) , are no longer fitting variables. They are inputs, at various energies. We found that the K^+/π^+ ratio calculated in generic (non)extensive statistics excellently reproduces the experimental results, including the horn–like structure. The nonmonotonic energy–dependence of $\gamma_{q,s}$ and that of (c, d) together are essential. We conclude that the excellent reproduction of the K^+/π^+ ratio requires:

1. Lambert– W_0 exponentially generated distribution rather than BG or Tsallis and
2. partial– or full–chemical nonequilibrium occupation factors.

With this regard, we assure you that other ratios such proton–to–pion are also perfectly reproduced, Appendix C.

While both partial– and full–chemical nonequilibrium in generic (non)extensive statistics seem to excellently reproduce the measured K^+/π^+ ratio, at all energies, the full–chemical

nonequilibrium is likely significant, at $3 \lesssim \sqrt{s_{NN}} \lesssim 10$ GeV. To refine the conclusion whether partial- or full-chemical nonequilibrium is essential for the nonmonotonic horn-structure of the K^+/π^+ ratio, a detailed beam energy scan by the STAR and CBM experiments, for instance, is highly recommended.

A. Probability distribution, entropy, exponential and logarithm functions in Boltzmann, Tsallis and generic (non)extensive statistics

For a reliable comparison between Boltzmann, Tsallis, and generic (non)extensive statistics, we first recall the corresponding probability distributions

$$\text{Extensive BG : } p_i(x) = \frac{\exp(-x)}{\mathcal{Z}(x)} = \frac{1}{\mathcal{Z}(x)} \sum_{n=0}^{\infty} \frac{x^n}{n!}, \quad (\text{A1})$$

$$\begin{aligned} \text{Nonextensive Tsallis : } p_i^{(q)}(x) &= \frac{\exp^{(q)}(-x)}{\mathcal{Z}^{(q)}(x)} = \frac{1}{\mathcal{Z}^{(q)}(x)} \left[1 - x + \frac{q}{2}x^2 - \frac{q^2}{3!}x^3 + \dots \right] \\ &= \frac{1}{\mathcal{Z}^{(q)}(x)} \left[1 + \sum_{n=1}^{\infty} \frac{x^n}{n!} Q_{n-1}(q) \right] = \frac{1}{\mathcal{Z}^{(q)}(x)} [1 + (1-q)x]^{1/(1-q)}, \end{aligned} \quad (\text{A2})$$

$$\begin{aligned} \text{(Non)extensive : } p_i^{(c,d,r)}(x) &= \frac{\exp^{(c,d,r)}(-x)}{\mathcal{Z}^{(c,d,r)}(x)} \\ &= \frac{1}{\mathcal{Z}^{(c,d,r)}(x)} \exp \left[\frac{-d}{1-c} \left\{ W_k \left[B \left(1 - \frac{x}{r} \right)^{1/d} \right] \right\} - W_k[B] \right], \end{aligned} \quad (\text{A3})$$

where $\mathcal{Z}(x)$ is the corresponding canonical partition function, $Q_{n-1}(q) := \Pi_{i=0}^n [iq - (i-1)]$ [48], and the asymptotic expansion of 0-th branch Lambert- W_k function is given as

$$W_{k=0}(x) = \sum_{n=1}^{\infty} (-1)^{n-1} \frac{n^{n-1}}{n!} x^n.$$

The probability distribution function can be obtained from the integral of the probability density function determining the probability of an individual *event* to take place in a given interval. Also, The probability distribution function can be derived from the maximization of the corresponding entropy under appropriate constraints

$$\text{Extensive BG : } s[p] = -\kappa \sum_{i=1}^{\Omega} p_i \ln p_i, \quad (\text{A4})$$

$$\text{Nonextensive Tsallis : } s^{(q)}[p] = \frac{\kappa}{1-q} \sum_{i=1}^{\Omega} \left(p_i^{(q)} - p_i \right),$$

$$\text{(Non)extensive : } s^{(c,d,r)}[p] = \kappa \sum_{i=1}^{\Omega} [\mathcal{A} \Gamma(d+1, 1-c \log p_i) - \mathcal{B} p_i], \quad (\text{A5})$$

where Ω is the number of micro-states or processes. κ , \mathcal{A} , and \mathcal{B} are arbitrary parameters. The incomplete gamma-function is given as [49]

$$\Gamma(a, x) = \int_x^\infty dt t^{a-1} \exp(-t) = \Gamma(a) - \frac{x^a}{a \exp(x)} \sum_{i=0}^{\infty} \frac{x^i (a)!}{(a-i)!}. \quad (\text{A6})$$

The differences between Boltzmann, Tsallis and generic (non)extensive statistical statistics can be characterized by the mathematical meaning of the corresponding exponential and logarithm functions; namely for Boltzmann $\exp(x)$ and $\ln(x)$, for Tsallis $\exp^{(q)}(x)$ and $\ln^{(q)}(x)$, and for generic (non)extensive functions $\exp^{(c,d,r)}(x)$ and $\ln^{(c,d,r)}(x)$. For example, the Tsallis exponential and logarithm functions, respectively read [50],

$$\begin{aligned} \exp^{(q)}(-x) &= 1 + \sum_{n=1}^{\infty} (-1)^n \frac{q^{n-1}}{n!} x^n = 1 - x + \frac{q}{2!} x^2 - \frac{q^2}{3!} x^3 + \dots, \\ \ln^{(q)}(x) &= \sum_{n=1}^{\infty} (-1)^{n+1} \frac{q^{n-1}}{n} (x-1)^n = (x-1) - \frac{q}{2} (x-1)^2 + \frac{q^2}{3} (x-1)^3 - \dots. \end{aligned} \quad (\text{A7})$$

For generic (non)extensive exponential and logarithm functions, generalization of BG $\exp(x)$ and $\ln(x)$ gives [51]

$$\exp^{(c,d,r)}(-x) = \exp \left\{ \frac{-d}{1-c} \left[\mathbb{W}_k \left(B (1-x/r)^{1/d} \right) - \mathbb{W}_k(B) \right] \right\}, \quad (\text{A8})$$

$$\ln^{(c,d,r)}(x) = r \left\{ 1 - x^{c-1} \left[1 - \frac{1-r(1-c)}{d r} \log(x) \right]^d \right\}. \quad (\text{A9})$$

It is now in order to comment on the interpretations of the Tsallis nonextensivity parameter q . First, the assumption that $q > 1$ manifests fluctuations in $1/\lambda$ of the so-called Levy exponential distribution, $\exp(-x/\lambda)$, is apparently superficial [52]. The nature of such fluctuations wasn't determined, yet. On the other hand, such fluctuations should be also accompanied by a remarkable change in the phase space, itself [11]. Likewise, we assess the connection between the departure of q from its extensive value, the unity, from above and the large fluctuations of temperature. Second, the claim on the existence of fundamental differences between BG- and Tsallis-statistics⁸ leads to an *ad hoc* prerequisite that the thermodynamic temperature, the one deduced from BG statistics, differs from the one determined in Tsallis statistics, $T_{Tsallis} = T_{BG} + (q-1)K$, where the parameter K should be modeled as a function of the energy transfer between the source and the surrounding [28]. This *phenomenological* interpretation is

⁸ There is no fundamental difference between BG- and Tsallis-statistics, unless the ealier is extensive and the latter is nonextensive statistical framework!

closely related to blind improper implementation of Tsallis–algebra⁹. It is worthy highlighting that the reproduction of the transverse momentum distributions was misinterpreted and accordingly the resulting temperature [53].

The present script suggests that Boltzmann and Tsallis statistics are subdomains of generic (non)extensive statistics. The Tsallis nonextensive parameter q is also included in BG; $q = 1$, as well as in generic (non)extensive statistics; $c = 0$ and $d = q$. The equivalence classes (c, d) are intrinsic properties of the entire statistical space, where $(c, d) = (1, 1)$ characterize Boltzmann statistics and $(c, d) = (0, q)$ represents the Tsallis type. The thermodynamic quantities either intensive or extensive, such as temperature, entropy, pressure, and energy density, should remain identical in the entire statistical space, i.e., they shouldn't be changing when moving from BG to Tsallis or to any other type of nonextensive statistics. The interpretations of q and of (c, d) aren't just dummy fluctuations but rather nonextensive statistical characterizations. Their nature is related to the properties of the relevant statistical ensemble.

B. Inclusion of very high–mass resonances and missing states in the hadron resonance gas model

The authors of ref. [54] introduced two ingredients to the extensive additive equilibrium hadron resonance gas model. The first one is very high–mass resonances (> 2 GeV). The second one is the σ meson or $f_0(600)$. The various decay channels are also taken into consideration.

The σ meson is characterized by energy–depending mass and varying decay constants. Its dominant decay channel produces pion pair. This might be the motivation of ref. [54]. Accordingly, it has been estimated that σ meson comes up with about 3.5% enhancement in the pion yields. The inclusion of very high–mass resonances also increase the pion yields, this time by about 13%. Enhancing pion yields against Kaon yields seems to reproduce the nonmonotonic K^+/π^+ ratio, on one hand. On the other, the standard of evidence prerequisites that the Kaon yields should be enhanced, similarly! Alternatively, the ensemble of the hadron resonances is left biased unbalanced.

Fig. 4 presents unbiased balanced reproduction of K^+/π^+ ratio (solid curve), where all hadrons and resonances reported in recent PDG, including σ meson and its heavier resonances [55], as well as 56 missing states are included in. Most if not all decay channels are also taken

⁹ Replacing $\exp(x)$ with $\exp_q(x)$, Eq. (A7) and $\ln(x)$ with $\ln_q(x)$, Eq. (A7)

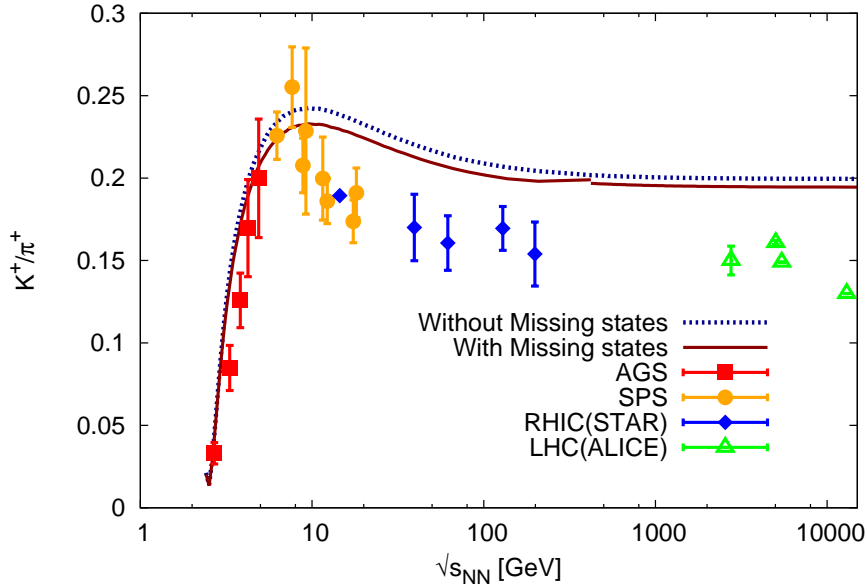


Fig. 4: Energy dependence of the relative production ratio K^+/π^+ measured at various energies. With the dotted curve, we show the K^+/π^+ ratio estimated in the hadron resonance gas model with extensive additive equilibrium BG statistics and dof determined by mass-truncated PDG compilation of hadrons and resonances. The solid curve shows the same but dof are the entire PDG compilation of hadron and resonances and up to 56 missing states.

into consideration, so that the final number of any particle is summed over that particle and all other decay channels producing it weighted with the corresponding decay width. The masses of the resonances can be as heavier as 12 GeV. We conclude that the inclusion of the very heavy-mass resonances would slightly enhance the respective particle yields, on one hand. On the other hand, such an enhancement is faded away in the relative production ratio. The K^+/π^+ ratio isn't well reproduced either with or without the inclusion of missing states.

The contributions of the missing states to the various thermodynamic quantities [46] are depicted in Fig. 5. At 7.7, 19.6, 39 and 200 GeV, the number density, energy density, and pressure calculated in the extensive additive equilibrium hadron resonance gas model, are compared with (symbols) and without (curves) missing states and when including (symbols) and excluding (curves) very-heavy mass resonances. We conclude that the inclusion of the missing states and very-heavy mass resonances minimally contributes to the particle yields. These contributions are apparently balanced in the relative particle production ratios, Fig. 4. With this regard, we recall that the authors of ref. [46] also have drawn the same conclusion that

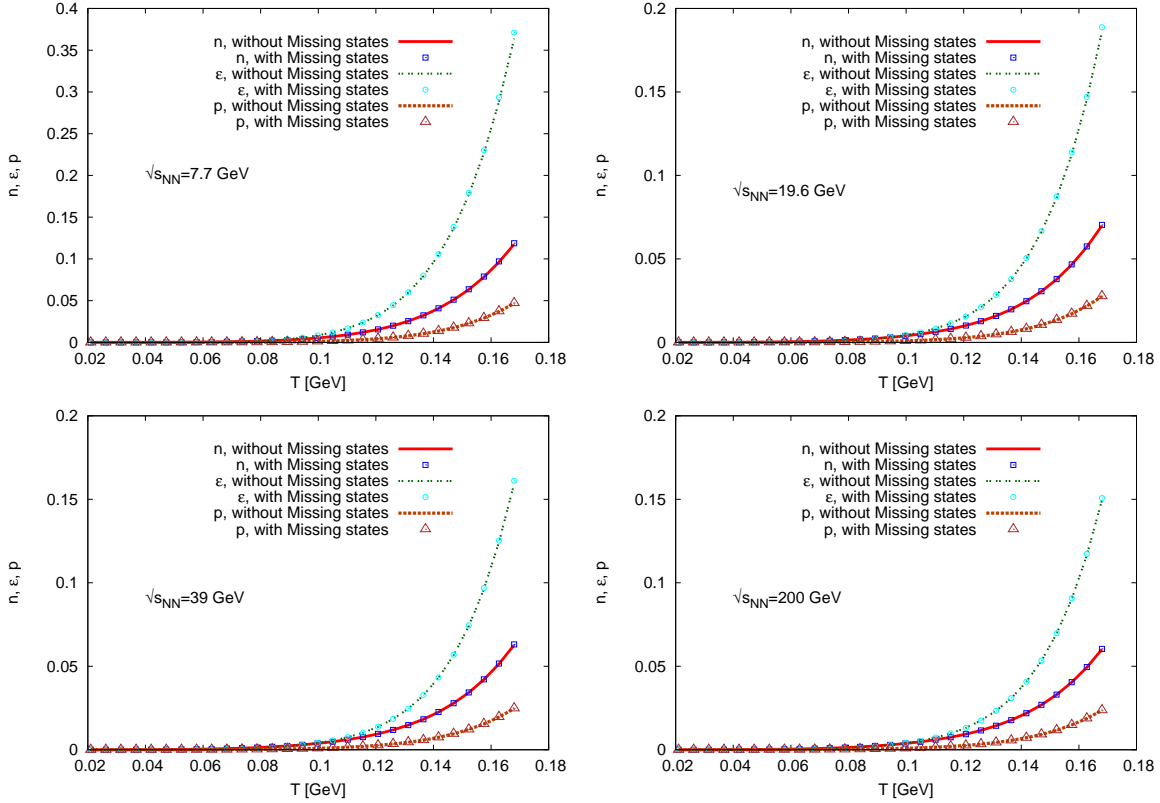


Fig. 5: Temperature dependence of number density, energy density and pressure calculated in the extensive additive equilibrium hadron resonance gas model, at 7.7, 19.6, 39 and 200 GeV. The curves show the results with truncated hadron mass spectrum, < 2 GeV. With the symbols, we show the results, where 56 missing states are included in and the hadron mass can be as heavy as 12 GeV.

”susceptibilities of conserved charges, [...] can be attributed to the missing resonances in the strange baryon sector.” In other words, the missing states become first dominant in the higher-order moments of conserved charges, such as susceptibilities and cumulants. But they slightly contribute to lower-order moments, such as the number density. Even this slight contribution is faded away in the particle ratios.

C. Contour plots of the quality of fits for $\gamma_{q,s}$

A suppression in γ_s was assumed as a signature of onset of the color deconfinement [25, 26]. The nonequilibrium quark occupation factors, $\gamma_{q,s} \neq 1$, are conjectured to dictate the numbers of light- and strange-quarks, respectively, which can be accommodated in the phase-space volume and accordingly the production rates of light and strange particle yields [8, 21, 22]. In all these

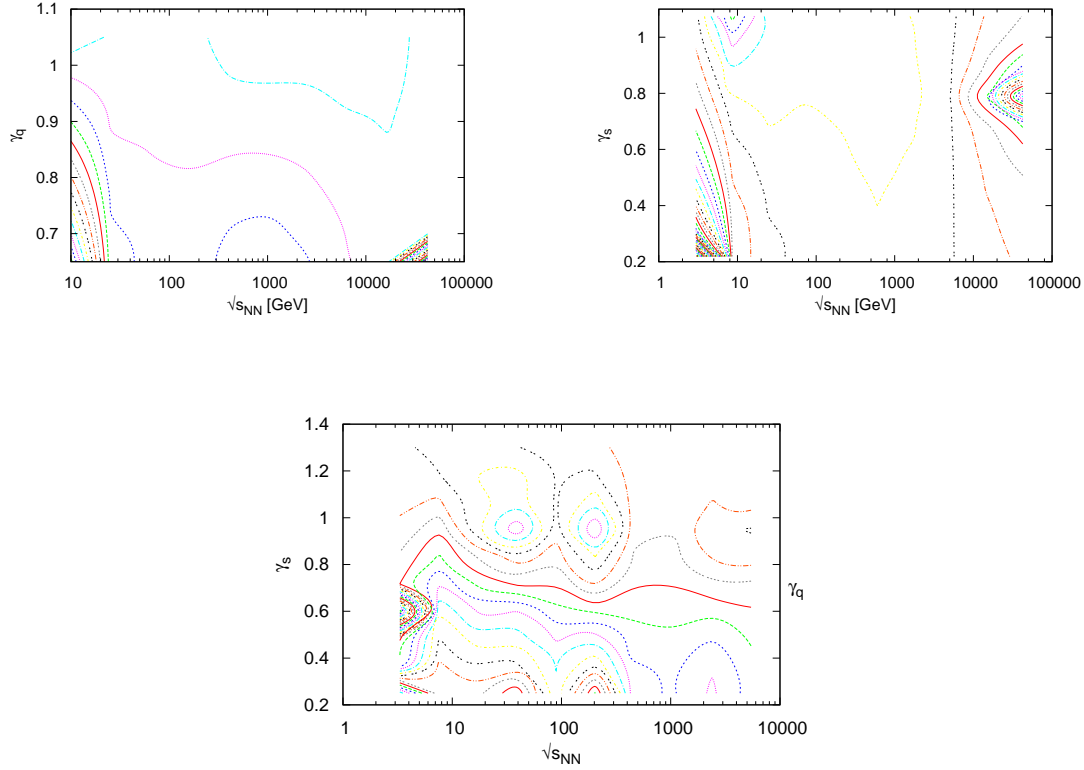


Fig. 6: Top left: contour plot of the quality of fit for γ_q , where $\gamma_s = 1$, over different collision energies. Top right: the same as in top left but for γ_s , where $\gamma_q = 1$. Bottom panel shows contour plot for nonequilibrium γ_q and γ_s , at different collision energies.

studies, extensive additive equilibrium BG statistics was utilized.

When γ_q is determined from the statistical fit of one particle ratio, the other particle ratios aren't well reproduced. Although various other particle ratios can simultaneously be reproduced for nonequilibrium $\gamma_{q,s}$, the resulting values of $\gamma_{q,s}$ are scattered, Table 1 of ref. [8]. Values of $\gamma_{q,s}$ much greater than unity are tough to incorporate with a nonequilibrium approach.

Figure 6 shows the contour plots of the quality of fits for γ_q (top left panel), γ_s (top right panel), and $\gamma_{q,s}$ (bottom panel). The resulting of $\gamma_{q,s}$ are parameterized in Eq. (9). When comparing with Table 1 of ref. [8], we conclude that the present estimations can be well incorporated with a nonequilibrium approach.

With the same sets of equivalence classes given by Eqs. (7)-(8) and nonequilibrium quark-occupation factors $\gamma_{q,s}$ given by Eq. (9), not only K^+/π^+ ratio is well reproduced, but other particle ratios, as well, for example, P/π^+ and Λ/π^- , Fig. 7. We like to highlight that at

> 4 TeV, the ensemble of the experimental results available so-far isn't large enough to deduce the equivalent classes. Thus, we have assumed that their results, at lower LHC energies, remain unchanged. There is a little overestimation, which can be improved with the release of LHC results in the near future.

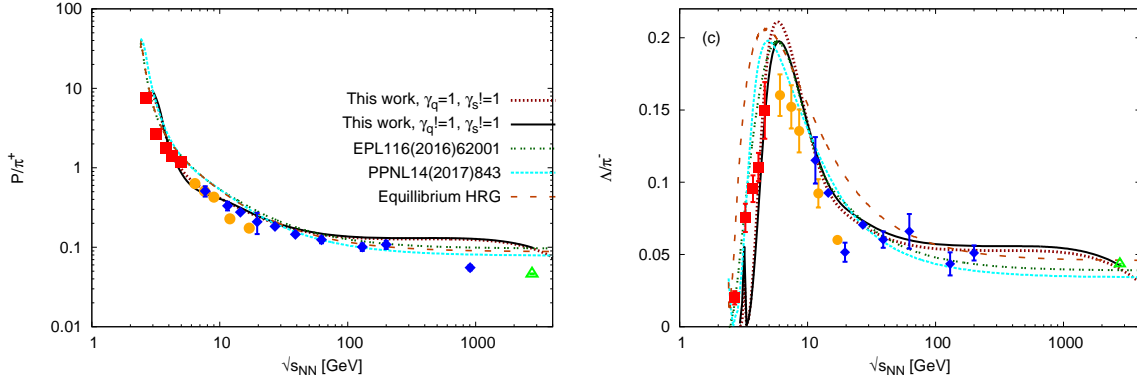


Fig. 7: Energy dependence of P/π^+ (left panel) and Λ/π^- (right panel), where the same sets of the equivalence classes are given by Eqs. (7)-(8) and $\gamma_{q,s}$ by Eq. (9), as the ones for K^+/π^+ are utilized.

-
- [1] M. Gazdzicki and M. I. Gorenstein, *Acta Phys. Polon. B* **30**, 2705 (1999).
 - [2] L. Ahle et al., *Phys. Lett. B* **476**, 1 (2000).
 - [3] I. G. Bearden et al., *Phys. Rev. C* **66**, 044907 (2002).
 - [4] S. V. Afanasiev et al., *Phys. Rev. C* **66**, 054902 (2002).
 - [5] M. Gazdzicki et al., *J. Phys. G* **30**, S701 (2004).
 - [6] J. Cleymans, H. Oeschler, K. Redlich, and S. Wheaton, *Eur. Phys. J. A* **29**, 119 (2006).
 - [7] A. Andronic, P. Braun-Munzinger, and J. Stachel, *Nucl. Phys. A* **772**, 167 (2006).
 - [8] A. Tawfik, *Fizika B* **18**, 141 (2009).
 - [9] B. Tomasik and E. E. Kolomeitsev, *Eur. Phys. J. C* **49**, 115 (2007).
 - [10] S. Chatterjee, R. M. Godbole, and S. Gupta, *Phys. Rev. C* **81**, 044907 (2010).
 - [11] A. Tawfik, *Prog. Theor. Phys.* **126**, 279 (2011).
 - [12] J. K. Nayak, S. Banik, and J.-e. Alam, *Phys. Rev. C* **82**, 024914 (2010).
 - [13] A. N. Tawfik, H. Yassin, and E. R. A. Elyazeed, Extensive/nonextensive statistics for p_T distributions of various charged particles produced in p+p and A+A collisions in a wide range of energies, 2019.

- [14] K. Shen, G. G. Barnaföldi, and T. S. Biró, *Universe* **5**, 122 (2019).
- [15] K. Shen, G. G. Barnaföldi, and T. S. Biró, *Eur. Phys. J. A* **55**, 126 (2019).
- [16] K. Shen, T. S. Biro, and E. Wang, *Physica A* **492**, 2353 (2018).
- [17] T. S. Biro, G. G. Barnafoldi, G. Biro, and K. M. Shen, *J. Phys. Conf. Ser.* **779**, 012081 (2017).
- [18] A. S. Parvan and T. S. Biro, *Phys. Lett. A* **375**, 372 (2011).
- [19] G. Wilk and Z. Wlodarczyk, *Acta Phys. Polon. B* **46**, 1103 (2015).
- [20] M. Rybczynski, Z. Wlodarczyk, and G. Wilk, *J. Phys. G* **39**, 095004 (2012).
- [21] A. N. Tawfik et al., *EPL* **116**, 62001 (2016).
- [22] A. N. Tawfik, H. Yassin, and E. R. Abo Elyazeed, *Phys. Part. Nucl. Lett.* **14**, 843 (2017).
- [23] A. N. Tawfik, *Int. J. Mod. Phys. A* **29**, 1430021 (2014).
- [24] A. Tawfik, *Phys. Rev. C* **88**, 035203 (2013).
- [25] P. Castorina, S. Plumari, and H. Satz, *Int. J. Mod. Phys. E* **26**, 1750081 (2017).
- [26] P. Castorina, S. Plumari, and H. Satz, (2018), [Addendum: *Int.J.Mod.Phys.E* 27, 1891001 (2018)].
- [27] A. N. Tawfik, H. Yassin, and E. R. Abo Elyazeed, *Indian J. Phys.* **92**, 1325 (2018).
- [28] A. Deppman, *J. Phys. G* **41**, 055108 (2014).
- [29] G. Bíró, G. G. Barnaföldi, T. S. Biró, and K. Ürmössy, *AIP Conf. Proc.* **1853**, 080001 (2017).
- [30] A. Nasser Tawfik, *Eur. Phys. J. A* **52**, 253 (2016).
- [31] R. Hanel and S. Thurner, *EPL* **93**, 20006 (2011).
- [32] A. N. Tawfik, *Phys. Part. Nucl. Lett.* **15**, 199 (2018).
- [33] R. Hanel and S. Thurner, *EPL* **936**, 50003 (2011).
- [34] A. Tawfik, *J. Phys. G* **40**, 055109 (2013).
- [35] J. Letessier and J. Rafelski, *Hadrons and Quark-Gluon Plasma*, UK:Cambridge University Press, 2004.
- [36] A. Tawfik, M. Y. El-Bakry, D. M. Habashy, M. T. Mohamed, and E. Abbas, *Int. J. Mod. Phys. E* **25**, 1650018 (2016).
- [37] A. Tawfik, *Adv. High Energy Phys.* **2013**, 574871 (2013).
- [38] A. Tawfik, *Europhys. Lett.* **75**, 420 (2006).
- [39] T. Nonaka, *JPS Conf. Proc.* **26**, 024007 (2019).
- [40] L. Adamczyk et al., *Phys. Rev. C* **93**, 021903 (2016).
- [41] J. Adams et al., *Nucl. Phys. A* **757**, 102 (2005).

- [42] B. Abelev et al., Phys. Rev. Lett. **109**, 252301 (2012).
- [43] J. Adam et al., Phys. Rev. C **101**, 024905 (2020).
- [44] S. Acharya et al., Eur. Phys. J. C **81**, 584 (2021).
- [45] S. Acharya et al., Phys. Rev. C **101**, 044907 (2020).
- [46] P. Man Lo, M. Marczenko, K. Redlich, and C. Sasaki, Eur. Phys. J. A **52**, 235 (2016).
- [47] A. N. Tawfik, M. A. Wahab, H. Yassin, E. R. Abo Elyazeed, and H. M. Nasr El Din, Int. J. Mod. Phys. E **26**, 1750046 (2017).
- [48] E. P. Borges, J. Phys. A **31**, 5281 (1998).
- [49] R. J. A. L. Pereira, M. A. Senra, and G. A. da Cruz, Natural Science **2012**, 919 (2012).
- [50] S. Umarov, C. Tsallis, and S. L. Steinberg, Milan Journal of Mathematics **76**, 307 (2008).
- [51] A. N. Tawfik, PoS **ICHEP2016**, 1153 (2017).
- [52] G. Wilk and Z. Wlodarczyk, Phys. Rev. Lett. **84**, 2770 (2000).
- [53] A. Bialas, Phys. Lett. B **747**, 190 (2015).
- [54] A. Andronic, P. Braun-Munzinger, and J. Stachel, Phys. Lett. B **673**, 142 (2009), [Erratum: Phys.Lett.B 678, 516 (2009)].
- [55] P. Zyla et al., PTEP **2020**, 083C01 (2020).